Chem. Res. Chin. Univ., 2017, 33(2), 312—317 doi: 10.1007/s40242-017-6262-3

Influence of Thermal Temperature on the Structure and Sealed Micropores of Stabilized Polyacrylonitrile Fibers

ZHAO Ruixue[1], ZHAO Xudong[1], GAO Zhongmin[1*], LIU Xiaoyang[1] and CHE Xiaolei[2*]

1. State Key Laboratory of Inorganic Synthesis and Preparative Chemistry, College of Chemistry, Jilin University, Changchun 130012, P. R. China;

2. College of Physics, Jilin University, Changchun 130012, P. R. China

Abstract Thermal stabilization is an important process in carbon fibers' production, during which the polyacrylonitrile fibers are heated from 180 °C to 280 °C in air. In this study, the samples were characterized by X-ray diffraction, Fourier infrared spectroscopy, differential scanning calorimetry, small angle X-ray Scattering(SAXS) and mechanical tensile tests. A new rule was suggested by the results of structural characterization for the cyclization, dehydrogenation and oxidation reactions that were observed to be drastic from 200 °C to 220 °C, from 220 °C to 250 °C, and in the later period of the thermal stabilization reactions, respectively. The sizes, shapes and distributions of the sealed micropores were obtained from the SAXS data. The breaking elongation was significantly affected by the drastic cyclization and dehydrogenation reactions. The breaking force was affected considerably by the bigger micropores, especially from 220 °C to 250 °C, owing to the drastic dehydrogenation reactions.

Keywords Polyacrylonitrile fiber; Thermal stabilization; Micropore

1 Introduction

Polyacrylonitrile(PAN) carbon fibers have excellent mechanical properties, good chemical and high temperature inertness and a low mass-to-volume ratio, resulting in increasingly wide applications in many areas, such as national defense(*e. g*., aerospace industry, military aircraft, and arms defense), business areas and civil engineering(*e. g*., sporting, transportation industry, architecture industry, and medical sectors)[1,2]. PAN fibers can be turned into carbon fibers through three thermal treatment stages[3]. The first stage is the stabilization stage at a temperature range from 200 °C to 300 °C, where cyclization, dehydrogenation and oxidation reactions occur and the linear structure of PAN is converted to an intermediate cyclic structure, which is critical in the second carbonization stage and the third graphitization stage[4]. Ozbek *et al*.[5] reported that three processing variables, including thermal treatment temperature, dwell time and tensile stress, significantly affected the quality of stabilized PAN based fibers, which further affected the performance and production ratio of carbon fibers.

The strength and performance of carbon fibers depend on many factors, such as composition, structure, and micropores, among which the sealed micropores are especially important. To date, several structural models have been proposed in order to understand the relationship between the mechanical properties and the structure. Johnson *et al*.[6] presented a structure model, in which the microcrystals were separated by the boundaries and micropores. Bennet *et al*.[7] presented a two-dimensional stripe structure model, in which the micropores formed among the stripes. Barnet *et al*.[8] presented a structure model of high modulus carbon fibers, in which the skin-core structure, crack, and micropores were included. From all the structure models, we can conclude that the sealed micropores are the key factor to building them. The sizes, shapes and distributions of the sealed micropores should be considered in the model and they are basically inherited from the thermal stabilization of PAN fibers. However, due to the complexity of the PAN fibers, it is challenging to directly measure the distributions of the sealed micropores by scanning electron microscopy(SEM) or transmission electron microscopy(TEM) in several sections of the fiber. In addition, the polymer like PAN precursor and stabilized PAN based fibers are easily damaged after the electron microscope treatment. Therefore, there have been some reports on the processing variables in the stabilization of PAN fibers, but few reports on the sealed micropores' change during stabilization.

In this paper, PAN fibers were treated in a temperature range of from 180 °C to 280 °C in order to study the reactions, the structural evolution and the sealed micropore change during the stabilization with thermal treatment temperatures. The reactions and the structure evolution were examined by X-ray diffraction(XRD), Fourier infrared spectroscopy(FTIR) and differential scanning calorimetry(DSC). We used a method based on small angle X-ray scattering(SAXS) to characterize the sealed micropores in the fibers during the thermal stabilization progress, which was used in the analysis of micropores in

*Corresponding authors. E-mail: gaozm@jlu.edu.cn; chexl@jlu.edu.cn

Received June 22, 2016; accepted January 3, 2017.

Supported by the Special Foundation of State Major Scientific Instrument and Equipment Development of China (No.2012YQ24026407) and the Fund of the China Education Resource System(No.CERS-1-3).

carbon fibers. In the method, the axial ratio(ω=c/a) of long shaft radiuses to short shaft radiuses was used to characterize the pore shape, while the Hausdorff dimension, D, was used to characterize the roughness of the pore's surface[9—11]. The evolution of the micropores of the fibers was studied at different temperatures, which was correlated with the XRD and FTIR results. The final analysis of the micropore evolution could be beneficial to the fabrication of carbon fibers and theoretical models.

2 Experimental

2.1 Preparation of Stabilized PAN Fibers

Polyacrylonitrile terpolymer[P(AN-MMA-IA)], fed with approximately 3%(mass fraction) MMA and 1%(mass fraction) IA, was generously provided by Jilin Chemical Fibre Co., Ltd., China. The PAN fibers were stabilized under air atmosphere by heating from 180 °C to the ending temperatures at a rate of 5 °C/min through a constant stretching, then maintained at the end temperature for a period of time to obtain the final 8 samples, whose end temperatures were 180 °C(PAN-1), 200 °C (PAN-2), 220 °C (PAN-3), 240 °C (PAN-4), 250 °C(PAN-5), 260 °C(PAN-6), 270 °C(PAN-7), and 280 °C(PAN-8).

2.2 Characterization

The tailor-made specimen plates twined with stabilized fibers under different conditions were ready for XRD and SAXS. An X-ray diffractometer(XRD, Rigaku D/MAX-2550) with Cu $K\alpha$ radiation generated at 50 kV and 200 mA was used over the 2θ range of 5°—55° with a scanning step of 0.02° and a scanning speed of 5 °C/min. A small angle X-ray scatterometer(SAXS, Rigaku D/MAX-2550) with Cu $K\alpha$ radiation and an incident multilayer monochromatic parallel light film over a 2θ range of 0.08°—6° with a scanning step of 0.02° and a single count time of 10 s was used under vacuum. The Fourier transform infrared spectra(FTIR) were obtained on a Nicolet Impact 410 FTIR spectrometer in an attenuated total reflectance mode and in a range of approximately 400—4000 cm^{-1} using KBr pellet method. The samples were subjected to DSC analysis on a NETZSCH DSC 204 F1 thermal analyzer at temperatures between 40 and 320 °C with a heating rate of 7 °C/min under N_2 atmosphere. The mechanical tensile tests were conducted on a YG061 FQ electronic yarn strength tester with a gauge length of 100 mm and a strain rate of 30 mm/min; 10 measurements were collected and averaged for each sample.

3 Results and Discussion

3.1 X-Ray Diffraction Analysis

The XRD patterns of PAN fibers stabilized at different temperatures from 180 °C to 280 °C are shown in Fig.1. For the PAN fibers, there are two strong characteristic peaks at 2θ of about 17.0° and 29.6° corresponding to the (100) and (110) planes, respectively. In addition, their crystalline interplanar spacings calculated by the Bragg equation are 0.513 and 0.30 nm, respectively[12—14]. The intensities of the two original peaks become weaker with the increasing of the stabilization temperature and almost disappear at relatively high temperatures. In addition, a new peak appears at 2θ of about 25.5° as the temperature increases, indicating that some microstructural evolution occurs at the thermal stabilization stage and the linear structure of PAN has been converted to an intermediate cyclic structure similar to the (002) plane of graphite structure[15,16].

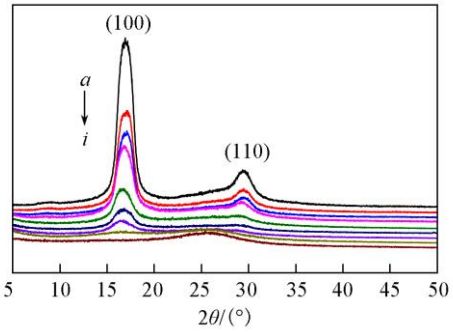

Fig.1 XRD patterns for PAN precursor(*a*) and stabilized PAN fibers(*b*—*h*)

b. PAN-1; *c*. PAN-2; *d*. PAN-3; *e*. PAN-4; *f*. PAN-5; *g*. PAN-6; *h*. PAN-7; *i*. PAN-8.

The crystallite sizes(L_c) were calculated from the Bragg equation and the Scherrer equation:

$$L_c = \frac{k\lambda}{B\cos\theta} \tag{1}$$

where λ(0.15418 nm) is the wavelength of Cu $K\alpha$ X-ray, θ is the Bragg angle, B is the full width at half maximum intensity(FWHM) of the peak(100) at approximately 2θ of 17.0°, and k is a constant with a value of 0.89. The crystallinity(C) of the fibers was determined by Hinrichsen's method[17]:

$$C(\%) = \frac{A_c}{A_a + A_c} \times 100\% \tag{2}$$

where A_c is the integral area of the crystalline zone at approximately 2θ of 17.0°, and A_a is the integral area of the amorphous zone in XRD patterns(A_c was calculated using the straight line segments from 2θ=11.0° to 2θ=21.0° as the baseline, while the total integral area A=A_a+A_c was calculated using the straight line segments from 2θ=11.0° to 2θ=32.0° as the baseline). The stabilization index(SI) value[18] was estimated using the following equation:

$$\mathrm{SI}(\%) = \frac{I_0 - I_i}{I_0} \times 100\% \tag{3}$$

where I_0 is the intensity of peak at 2θ of about 17.0° from the PAN precursor fibers, and I_i is the intensity of the peak at 2θ of about 17.0° from the stabilized fibers(all the samples' peak intensities were normalized with the same standard). The data are shown in Table 1.

The intensity of the peak at 2θ of about 17° becomes weaker with the increasing of the temperature, indicating that some microstructural evolution has occurred, and a new intermediate cyclic structure has been generated. The SI value characterizes the stabilization to a degree. From Table 1, we can see that the SI value increases as the temperature increases, particularly from 220 °C to 250 °C, indicating that the

stabilization degree increases with the increasing temperature. When the temperature reaches 280 °C, the SI value is 98.88%, indicating the near completion of the stabilization reaction. Owing to the constant tensile stress, the L_c decreases as the temperature increases, suggesting that stabilization progress is a grain refining process[19]. L_c and C clearly decrease from 200 °C to 220 °C, corresponding to a sudden peak position shift from 16.939° to 16.814° in the XRD patterns, which depends on the structure's expansion resulted from the drastic cyclization reactions in the above mentioned temperature range. L_c changes little from 220 °C to 250 °C, indicating that the dehydrogenation reactions occurring mainly in this temperature range rarely affect the crystallite size. Although L_c and C decrease as the temperature increases, they change faster after 250 °C, demonstrating that the oxidation reactions are drastic during the later period of the thermal stabilization reaction.

Table 1 XRD data for the PAN precursor and stabilized PAN fibers

Fiber	Peak intensity/a.u. (2θ *ca.* 17°)	L_c/nm	C(%)	SI(%)
PAN precursor	8018	4.56	62.29	—
PAN-1	4779	4.28	64.23	40.40
PAN-2	3994	4.26	60.80	50.19
PAN-3	3373	3.60	51.12	57.93
PAN-4	1635	3.55	44.40	79.61
PAN-5	976	3.63	43.74	87.83
PAN-6	603	3.31	30.55	92.48
PAN-7	186	2.90	10.04	97.68
PAN-8	90	2.83	5.52	98.88

3.2 Fourier Infrared Spectroscopy Analysis

Fig.2 shows the FTIR spectra of the PAN precursor and the stabilized PAN fibers. For the PAN precursor, the peaks at 2245 cm^{-1} could be attributed to the stretching vibration of C≡N; the peak at 1620 cm^{-1} could be attributed to the stretching vibrations of C═N and C═C; the peak at 1735 cm^{-1} is attributed to the C═O stretching from the itaconic acid(1%, mass fraction); the peaks at 1451, 1358 and 2938 cm^{-1} are resulted from the bending vibration of methylene groups(CH_2) and the stretch vibration of methylene groups(CH_2). There are almost no changes in the spectra of PAN-1 and PAN-2(180 and 200 °C), which means that no obvious chemical reactions have occurred. The intensity of the peak at 1735 cm^{-1} gradually decreases, and finally disappears as the temperature increases to 220 °C, which indicates that the cyclization is significantly accelerated by the temperature and initiated *via* an ionic mechanism with the decrease of the itaconic acid inherited from the precursor[20]. The decrease of the stretching vibration intensity of C≡N at 2245 cm^{-1} from 200 °C to 220 °C is more obvious, indicating that the cyclization reactions are drastic, corresponding to the XRD analysis. Three peaks at 1451, 1358 and 2938 cm^{-1} suddenly decrease at 220 °C accompanied by the disappearance of the itaconic acid, indicating that the dehydrogenation reactions become more and more drastic. It can also be seen that the bands at 1735 and 1620 cm^{-1} shift left and gradually combine into a shoulder-like peak at approximately 1660 cm^{-1}. It can be concluded that the shoulder-like peak corresponds to the mixing groups of C═C, C═N and C═O owing to the drastic oxidation reactions[21—23]. All these changes indicate that some conjugation structures are gradually generated.

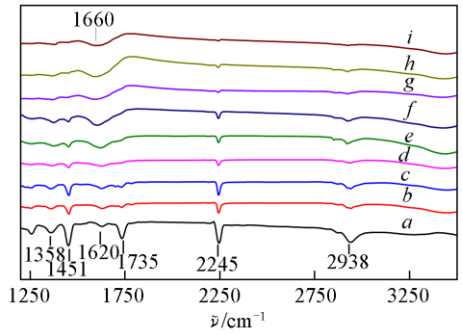

Fig.2 FTIR spectra for PAN precursor(*a*) and stabilized PAN fibers(*b*—*i*)

b. PAN-1; *c*. PAN-2; *d*. PAN-3; *e*. PAN-4; *f*. PAN-5; *g*. PAN-6; *h*. PAN-7; *i*. PAN-8.

3.3 X-Ray Photoelectron Spectroscopy Analysis

To study the structural formation, the XPS measurements of the PAN precursor and stabilized PAN fibers were performed, and the XPS patterns for C_{1s}, N_{1s} and O_{1s} are shown in Fig.3. For PAN-1, the broadening of C_{1s}, N_{1s} and O_{1s} binding energy demonstrates that the molecular structure of the fibers becomes looser because of the physical changes during heating at 180 °C[9]. For the C_{1s} XPS opattern of PAN-3, the binding energy ratio of the main peak to that of the shoulder peak clearly increases, compared with that of the PAN-2 fibers, and the relevant N_{1s} and O_{1s} binding energies also increase, which all indicate that the cyclization reactions are drastic from 200 °C to 220 °C[10]. The broadening of C_{1s}, N_{1s} and O_{1s} binding energies for the PAN-4 fibers also suggest that the molecular structure of PAN fibers becomes looser, indicating that the dehydrogenation reactions are drastic. And when the temperature reaches 250 °C(PAN-5 fibers), the dehydrogenation reactions are nearly over. More —C═O and ═N—O— structures have been generated in the PAN-7 fibers as the drastic oxidation reactions make the structures unstable, leading to the increasing and broadening of the binding energy, indicating that the oxidation reactions are drastic during the later period of the

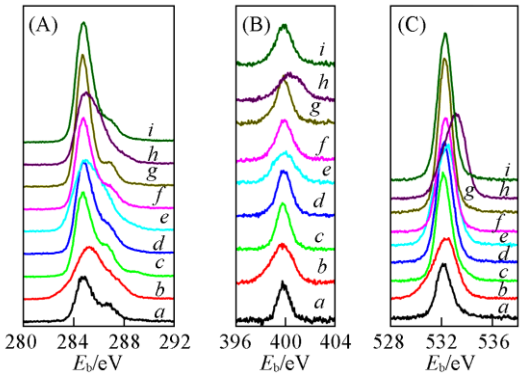

Fig.3 XPS curves of PAN precursor(*a*) and stabilized PAN fibers(*b*—*i*)

(A) C_{1s}; (B) N_{1s}; (C) O_{1s}. *b*. PAN-1; *c*. PAN-2; *d*. PAN-3; *e*. PAN-4; *f*. PAN-5; *g*. PAN-6; *h*. PAN-7; *i*. PAN-8.

thermal stabilization reactions[11]. Because of the drastic oxidation reactions, the molecular structure of PAN-7 fibers become looser and then is stabilized when the temperature increases to 280 °C.

3.4 Differential Scanning Calorimetry Analysis

Under the conditions of N_2 and no oxidative reactions occurring, the DSC exotherms of the PAN precursor and stabilized PAN fibers could be attributed to the cyclization reactions[21]. In Fig.4, there are no exothermic peaks for the stabilized PAN fibers after 220 °C in the temperature range of 200—320 °C due to the cyclization reactions, which can cause a large amount of heat to be released. This phenomenon results in the breakage of molecular chains giving off volatile components that makes the quality of the resultant fibers poor. The peak for PAN-3 is broader than those of fibers PAN-1 and PAN-2, showing that the cyclization reactions are nearly completed and the sharply exothermic reactions are diluted to an extent, which is beneficial to making high-performance carbon fibers. The endothermic peak between 40 and 140 °C can be mainly attributed to the release of moisture. The PAN-4 fibers have greater release of moisture possibly due to the drastic dehydrogenation reactions. The PAN-7 and PAN-8 fibers have greater release of moisture due to the nearly completed thermal stabilization reactions, which leads to the higher oxygen content on the surface. Furthermore, the results of DSC curves are consistent with that of the FTIR spectra.

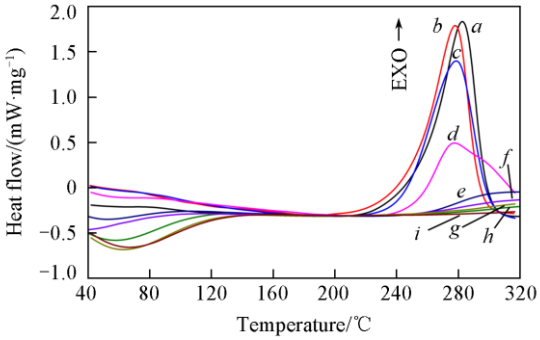

Fig.4 DSC curves of PAN precursor(*a*) and stabilized PAN fibers(*b*—*i*)

b. PAN-1; *c*. PAN-2; *d*. PAN-3; *e*. PAN-4; *f*. PAN-5; *g*. PAN-6; *h*. PAN-7; *i*. PAN-8.

3.5 Small Angle X-Ray Scattering Analysis

The sizes, shapes and distributions of the sealed carbon fiber micropores, which are evolved from the stabilization process of the PAN fibers, are the key factors to building the structure models to interpret these properties and are important to their mechanical properties[22,23]. In this approach, the sealed micropores of the stabilized PAN fibers were measured by the SAXS technique, and the patterns are shown in Fig.5. Due to the ellipsoid shape and the orientation of the sealed micropores, the fibers were measured along and vertical to the fiber axis direction, respectively, in order to obtain the long shaft radius(c) and the short shaft radius(a), respectively.

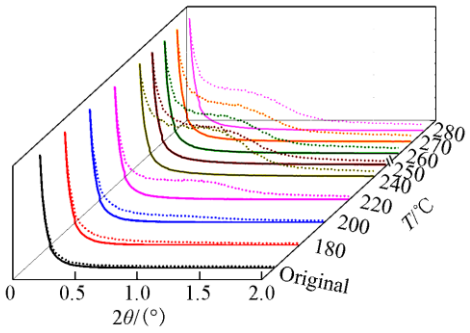

Fig.5 Scattering intensity curves measured along (solid lines) and vertical to(dotted lines) the fiber axis direction for the stabilized PAN fibers

According to the angle scattering theory: $I(h)=I_eNn^2\exp(-c^2h^2/5)$[where $I(h)$ is the scattered intensity, I_e is the intensity scattered by a single electron, $h(|h|=4\pi\sin\theta/\lambda)$ is the diffraction vector value, N is the total number of particles after X-ray irradiation, n is one particle's total number of electrons]. The long shaft radius(c) of the micropores can be obtained from the tangent slope(α_1) of the linear relationship of $\ln[I(h)]$ *vs.* h^2 using $c=(-5\alpha_1)^{1/2}$. The short shaft radius(a) can be obtained in a similar way, and the ratio of the long shaft radius(c) to the short shaft radius(a) is named as ω.

It is almost impossible to calculate the intensity for every radius of the micropores, but the intensity could be fitted with several radii and percentages, which could subsequently be treated as the fitting parameters. Each group of parameters demonstrates that there are specific percentages(or contents) of the micropores whose radii are around a specific radius. The SAXS data were fitted with four parameter groups($\omega=c/a$, φ, volume ratio, %): the ω of the pores whose cross sectional areas are between 2π and 10π nm^2 is ω_1; the ω of the pores whose cross sectional areas are between 10π and 100π nm^2 is ω_2; the ω of the pores whose cross sectional areas are between 100π and 300π nm^2 is ω_3; the ω of the pores whose cross sectional areas are more than 300π nm^2 is ω_4. All the ω data are listed in Table 2. The pore shape was similar to an elliptic ball if ω was small, and the pore shape was similar to a long rod or needle if ω was large[24,25].

To investigate the influence of the roughness of the pore surface on the mechanical properties, the Hausdorff dimension, D(between 2 and 3), was introduced to characterize the roughness. The larger the D became, the rougher the pore surface was. SAXS is often used to measure the Hausdorff dimension. Bale *et al.*[26] derived the formula for the small angle X-ray scattering intensity:

$$I(h)=\pi N_0\Delta\rho^2 I_0\Gamma(5-D)\sin[\pi(D-1)/2]h^{D-A} \quad (4)$$

where D is the Hausdorff dimension, h is the diffraction vector value, $I(h)$ is the scattering intensity, $\Delta\rho$ is the electron density difference value, $\Gamma(5-D)$ is a function, N_0 is a constant, A is the constant 5[26,27]. According to this formula, the Hausdorff dimension, D, can be obtained by calculating the tangent slope of the relationship between $\ln[I(h)]$ and $\ln h$. The obtained axis ratios(ω), volume ratios(φ, %) and fractal dimensions(D) of the sealed micropores in different PAN fibers treated at different temperature are listed in Table 2, while the trends for axis

Table 2 Axis ratios(ω), micropores volume ratios(φ, %) and fractal dimensions(D) for the PAN precursor and stabilized PAN fibers

Sample	Original	PAN-1	PAN-2	PAN-3	PAN-4	PAN-5	PAN-6	PAN-7	PAN-8
ω_1	3.32	1.50	1.18	2.58	2.24	2.18	2.06	1.96	1.92
ω_2	2.79	2.40	1.54	1.13	1.13	1.06	1.09	1.07	1.10
ω_3	3.11	2.59	1.75	3.11	3.43	2.14	2.42	2.61	2.74
ω_4	3.24	2.56	1.80	2.51	3.25	1.93	2.36	2.63	2.75
φ_1(%)	74.96	84.19	81.60	93.14	91.31	89.90	91.10	92.42	93.57
φ_2(%)	11.64	5.33	6.58	4.97	7.18	7.84	6.57	5.81	4.87
φ_3(%)	7.43	5.12	4.78	0.96	0.77	1.25	1.23	1.08	0.97
φ_4(%)	5.96	5.35	7.04	0.93	0.74	1.01	1.10	0.68	0.59
D	2.13	2.30	2.61	2.76	2.89	2.93	2.95	2.92	2.94

ratios(ω), micropore volume ratios(φ, %, V/V_4) and fractal dimensions(D) are plotted in Fig.6.

During thermal stabilization, the fibers shrink because of cyclization and oxidation, thus stretching is needed to maintain the shape of the fibers and is often accompanied by the generation of large numbers of micropores. The sizes, shapes and distributions of these micropores are crucial for the mechanical properties of the fibers. Some properties of these sealed micropores could be obtained from our fitting results of the SAXS measurements. The analysis of volume contents in Fig.6(B) shows that most of the micropores are small ones with the axis ratio being ω_1, whose cross sectional areas are between 2π and 10π nm^2. The analysis of the axis ratio in Fig.6(A) shows that the decreases in ω_1 from 180 °C to 200 °C and from 220 °C to 250 °C are due to the physical changes and dehydrogenation, respectively; and the increases from 200 °C to 220 °C and after 250 °C are due to the drastic cyclization reactions and oxidation reactions, respectively, based on the analysis of the XRD and FTIR measurements. As there are few changes for the largest micropores with ω_4 in the fibers, the quantity of the micropores was normalized by the contents of the micropores with ω_4. The results from Fig.6(D) show that the quantity of the micropores with ω_1 significantly increased after thermal stabilization, especially from 200 °C to 220 °C and after 250 °C, due to the cyclization and oxidation, respectively. The analysis of the Hausdorff dimension, D, in Fig.6(C) indicates that the D value gradually increases from 2 to 3 with the increase of stabilized temperature, which suggests that the pore surface is rougher and rougher. This increased pore surface roughness as a result of the increased temperature proves that the cyclization, dehydrogenation and oxidation reactions occurring in the generation of a new steady ladder polymer structure would affect the roughness of the pore surface. From the above analysis, we concluded that the micropores were significantly but irregularly affected by the chemical reactions[28—30], and the optimization of stretching, temperature and time of the thermal stabilization progress could help in obtaining high quality carbon fibers.

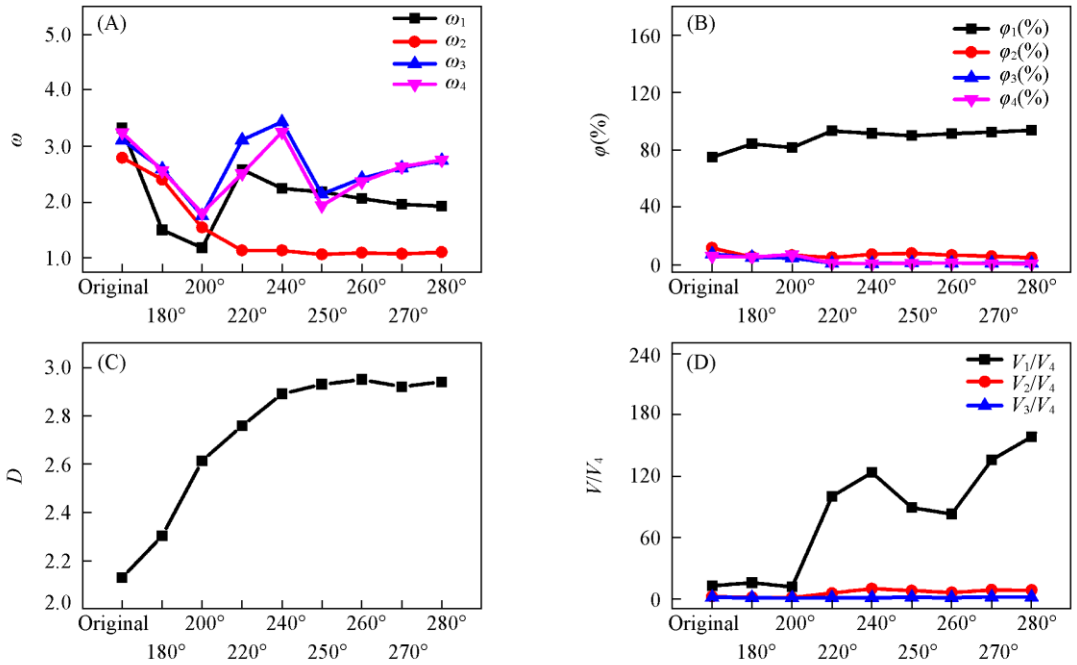

Fig.6 Trend charts for axis ratios ω(A), micropore volume ratios(φ, %, B), fractal dimension D(C) and the relative rate V/V_4(D)

3.6 Mechanical Tensile Tests

The mechanical tensile properties of the fibers are closely correlated to their sealed micropore changes. In Fig.7, we can see that the breaking force and breaking elongation increase from 180 °C to 200 °C with the decrease of ω in Fig.6 owing to

the physical change. The breaking force decreases little from 200 °C to 220 °C contrasting with the sharp increase of ω_1 and V_1/V_4 in Fig.6, which indicates that it is negligibly affected by the change in the smallest micropores, but affected significantly by the bigger micropores, whose V_3(%) and V_4(%) decrease in this range. The irregular and active shape change of the bigger micropores from 220 to 250 °C shown in Fig.6(A) makes the breaking force decrease rapidly owing to the drastic dehydrogenation reactions. However, the breaking force increases from 260 °C to 280 °C, which indicates that a new intermediate cyclic structure generated gradually and the breaking force would become much greater after the carbonization process. The breaking elongation decreases to a large extent from 200 °C to 250 °C, and then is stable after 250 °C, which indicates that it is affected little by the drastic oxidation reactions, but a lot by the drastic cyclization and dehydrogenation reactions. All the trends discussed above could be instructive for enhancing the mechanical performance of subsequent carbon fibers.

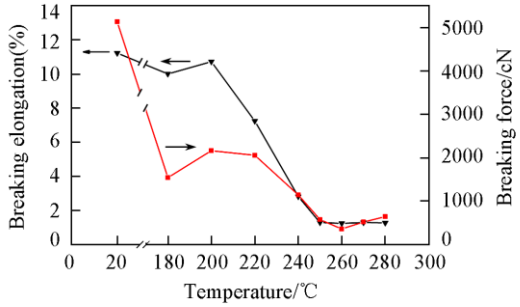

Fig.7 Mechanical tensile tests' trends chart for the PAN precursor and stabilized PAN fibers

4 Conclusions

The structure evolution and the sealed micropores of the stabilized polyacrylonitrile fibers studied by XRD, FTIR, DSC and SAXS demonstrated that the cyclization, dehydrogenation and oxidation reactions were drastic from 200 °C to 220 °C, from 220 °C to 250 °C, and in the later period of the thermal stabilization reaction, respectively. The thermal stabilization stage was complete at 280 °C, and a new intermediate cyclic structure was generated in this stage, which was similar to the (002) plane of graphite structure.

The sizes, shapes and distributions of the sealed micropores were obtained from the SAXS data. The results showed that most of the micropores had cross-sectional areas between 2π and 10π nm^2 with the axis ratio ω_1, the quantity of which significantly increased following thermal stabilization, especially from 200 °C to 220 °C and after 250 °C caused by cyclization and oxidation, respectively. The decrease of ω_1 from 180 °C to 200 °C and from 220 °C to 250 °C was due to the physical change and dehydrogenation, respectively, and the increase from 200 °C to 220 °C and after 250 °C was due to the drastic cyclization reactions and oxidation reactions, respectively, based on the analysis of the XRD and FTIR measurements. The results of the Hausdorff dimension, D, indicated that the surface of the micropores were rougher and rougher.

The breaking force was negligibly affected by the change in the smallest micropores but significantly affected by the larger micropores, particularly from 220 °C to 250 °C owing to the drastic dehydrogenation reactions. This value increased from 260 °C to 280 °C, which indicated that a new intermediate cyclic structure was gradually generated, and the breaking force would become much stronger after the carbonization progress. The breaking elongation was affected little by the drastic oxidation reactions but was affected strongly by the drastic cyclization and dehydrogenation reactions. Our analysis in this paper could be instructive for making high quality carbon fibers.

References

[1] Gao Y., Gao Z. M., Li X. S., Guo J. Q., Wen Y. F., Yang Y. G., *Chem. J. Chinese Universities*, **2009**, *30*(10), 2100
[2] Mun S. Y., Lim H. M., Lee D. J., *Thermochim. Acta*, **2015**, *600*, 62
[3] Gao Y., Huang K. K., Hua Z., Gao Z. M., Li X. S., *Chem. J. Chinese Universities*, **2007**, *28*(10), 2014
[4] He D. X., Wang C. G., Bai Y. J., Lun N., Zhu B., Wang Y. X., *J. Mater. Sci.*, **2006**, *42*(17), 7402
[5] Ozbek S., Isaac D. H., *Carbon*, **2000**, *38*, 2007
[6] Johnson D. J., Tyson C. N., *Br. J. Appl. Phys.*, **1969**, *2*(6), 787
[7] Bennett S. C., Johnson D. J., *Carbon*, **1979**, *17*(1), 25
[8] Barnet F. R., Norr M. K., *Carbon*, **1973**, *11*(4), 281
[9] Wang H. L., Zhao Y., Ma L. K., Fan P. H., Xu C. B., Jiao C. L., Lin A. J., *Chem. J. Chinese Universities*, **2016**, *37*(2), 335
[10] Wu B., Zheng G., Liu X. Z., Sun Y., Liu H. B., Zhu J. W., *Chem. J. Chinese Universities*, **2016**, *37*(10), 1891
[11] Chai X. Y., Zhu C. Z., He C. X., Zhang G. Z., Liu J. H., *Acta Physico-Chimica Sinica*, **2014**, *30*(4), 753
[12] Wu S. H., Qin X. H., *J. Therm. Anal. Calorim*, **2014**, *116*(1), 303
[13] Gupta A. K., Singhal R. P., Maiti A. K., Agarwal V. K., *J. Appl. Polym. Sci.*, **1982**, *27*, 4101
[14] Bhat G. S., Cook F. L., Abhiraman A. S., *J. Appl. Polym. Sci.*, **1990**, *28*, 377
[15] Loidl D., Paris O., Burghammer M., Rieke C., Peterlik H., *Phys. Rev. Lett.*, **2005**, *95*(22), 225501
[16] Xiao H., Lu Y. G., Zhao W. Z., *J. Mater. Sci.*, **2014**, *49*(2), 794
[17] Gupta V. B., Kumar S., *J. Appl. Polym. Sci.*, **1981**, *26*, 1885
[18] Shin H. K., Park M., Kang P. H., *J. Ind. Eng. Chem.*, **2014**, *41*(9), 6815
[19] Astrom J. A., Krasheninnikov A. V., Nordlund K., *Phys. Rev. Lett.*, **2004**, *93*(21), 215503
[20] Ju A. Q., Guang S. Y., Xu H. Y., *Carbon*, **2013**, *54*, 323
[21] Zhang W. X., Liu J., Wu G., *Carbon*, **2003**, *41*(14), 2805
[22] Cao F., Zhao L., *Chem. J. Chinese Universities*, **2011**, *32*(12), 2711
[23] Fu Z. Y., Gui Y., Cao C. L., Liu B. J., Zhou C., Zhang H. X., *J. Mater. Sci.*, **2014**, *49*(7), 2864
[24] Huang Z. F., Wang C. Z., Wei Y. J., *Chem. J. Chinese Universities*, **2004**, *25*(6), 1124
[25] Shioya M., Takaku A., *J. Appl. Phys.*, **1985**, *58*(11), 4074
[26] Bale H. D., Schmidt P. W., *Phys. Rev. Lett.*, **1984**, *53*(6), 596
[27] Benmore C. J., Izdebski T., Yarger J. L., *Phys. Rev. Lett.*, **2012**, *108*(17), 178102
[28] Kim H. S., Shioya M., Takaku A., *J. Mater. Sci.*, **1999**, *34*(14), 3307
[29] Li W., Long D., Miyawaki J., Qiao W., Ling L., Mochida I., Yoon S. H., *J. Mater. Sci.*, **2012**, *47*(2), 919
[30] Jain M. K., Abhiraman A. S., *J. Mater. Sci.*, **1987**, *22*(1), 278